Simultaneous magnetic and chemical order-disorder phenomena in Fe_3Ni, FeNi, and $FeNi_3$

M.-Z. Dang and D. G. Rancourt*
Department of Physics, University of Ottawa, Ottawa, Ontario, Canada K1N 6N5
(Received 24 July 1995)

We study the magnetic and chemical order-disorder transitions in face-centered-cubic $FeNi_3$, FeNi, and Fe_3Ni, by Monte Carlo (MC) simulations using the Ising approximation. The calculations are done: (1) with magnetic interactions only, assuming fixed preset degrees of chemical order, (2) with chemical interactions only, and (3) with both magnetic and chemical interactions acting simultaneously. As expected and known from measurements, the degree of chemical order is found to have a large influence on the magnetic transitions. On the other hand, although one might expect the effects of magnetism on the chemical ordering processes to be small (because the chemical bond energies are much larger than the magnetic exchange bond energies), one finds that the latter effects are also large. Several new features arise that are not predicted by mean-field theory or MC simulations with chemical interactions only. For example: (1) chemical order can be induced where using chemical interactions only leads to the prediction of no chemical order, (2) chemical segregation can be induced where using chemical interactions only leads to the prediction of no chemical segregation, (3) $FeNi_3$ and Fe_3Ni are found to have significantly different chemical ordering temperatures where chemical interactions only lead to equal ordering temperatures, (4) chemical ordering temperatures are significantly shifted from their chemical interactions only values, even when the chemical ordering temperature is larger than the magnetic ordering temperature (or Curie point), (5) abrupt steps can occur in the spontaneous magnetization at the chemical ordering temperature, when the latter is smaller than the magnetic ordering temperature, and (6) nonlinear relations arise between the chemical ordering temperature and the usual differential bonding parameter $U \equiv 2U_{\mathrm{FeNi}} - U_{\mathrm{FeFe}} - U_{\mathrm{NiNi}}$, where the U_{ij}'s are the near-neighbor pair-wise chemical bonds.

I. INTRODUCTION

The face-centered-cubic (fcc) Fe-Ni system, with Invar at ~65 at. % Fe and Elenvar at ~45 at. % Fe, has probably been the most studied binary transition-metal alloy series.[1] This is due to many factors such as Guillaume being awarded the Nobel prize for the discovery of Invar, the subsequent technological applications of Invar and Elenvar, the quest to understand Invar behavior at a fundamental level, the discovery of many associated properties originally known as Invar anomalies and that have now been observed in many other systems, and the importance of Fe-Ni alloys in Earth and planetary science (the earth's core and iron meteorites).

The ambient-pressure temperature composition structural phase diagram of Fe-Ni is complicated and is still being elaborated.[2,3] It includes: an Fe-rich body-centered-cubic (bcc) phase (α-phase), an fcc phase (γ-phase) that can be metastably quenched over a broad composition range (0–70 at. % Fe at room temperature; Invar and Elenvar are two such alloys), a low-spin fcc phase (γ_{LS}-phase), and chemically ordered fcc phases centered at ~50 and ~25 at. % Fe (FeNi and $FeNi_3$ phases, respectively). A chemically ordered Fe_3Ni fcc phase also has often been proposed but its existence has never been substantiated by firm experimental evidence. In addition, high-pressures stabilize a nonmagnetic hexagonal close-packed (hcp) phase[4–6] (ε-phase) that is closely related to the γ_{LS}-phase.[3]

Different models for the magnetism of the γ-phase have been proposed: two-γ-state model,[7–9] weak itinerant ferromagnetism,[10] latent antiferromagnetism,[11,12] etc. In all cases, the magnetism is believed to cause Invar behavior via some form of magnetovolume or magnetostructural coupling. Recently, it has been shown[13,14] that a simple local moment model with three composition-independent pair-specific near-neighbor (NN) magnetic exchange parameters (J_{FeFe}, J_{FeNi}, and J_{NiNi}) reproduces all of the main purely magnetic properties of the quenched γ-phase alloys: the Curie point versus composition, the spontaneous saturation moment versus composition, the spontaneous magnetization versus temperature at each composition, and the high-field (paraprocess) susceptibility at $T=0$ K versus composition.

Both cluster-method mean-field theory (MFT) calculations[13,15] and Ising approximation Monte Carlo (MC) simulations[14] were used. The MC simulations give superior agreement with experiment except for the paraprocess susceptibility where the Ising approximation of the MC simulations gives artificial steps, whereas the Heisenberg Hamiltonian of the MFT calculations gives realistic behavior with gradual spin rotation. The anomalies in all the magnetic properties are seen to arise from an antiferromagnetic NN Fe-Fe coupling ($J_{\mathrm{FeFe}}<0$) in these otherwise ferromagnetic alloys. Some magnetic frustration on the fcc lattice occurs at the Fe-rich end.

It follows that high-spin fcc (γ-phase) Fe-Ni alloys can be approximated as local moment systems with stable moments ($0.6\mu_B$ and $2.8\mu_B$ on Ni and Fe atoms, respectively) and NN-only Ising exchange interactions. This is particularly true at compositions $C \lesssim 50$ at. % Fe where the agreement between MC simulations and measurements is quantitative. In this paper, we assume that the same simple model of the magnetism (with the same NN J values) holds for the chemically ordered γ-phase counterparts (Fe_3Ni, FeNi, and $FeNi_3$) and include the chemical order-disorder process using NN-

only chemical bonds in our MC simulations.

In FeNi and $FeNi_3$ the degree of chemical order is known to have a significant effect on the measured magnetic properties and a previous MFT calculation[16] showed that magnetism measurably perturbs the $FeNi_3$ phase boundaries in the structural phase diagram. We now ask: How in detail does magnetism affect the chemical ordering processes? One might think that the effects should be very small because the chemical bond energies are much larger than the magnetic exchange bond energies. This however is incorrect: What matters is that the magnetic and chemical contributions to the change in energy on ordering are comparable. Indeed, we find large effects where the chemical and magnetic ordering processes are not simply mutually perturbed.

To our knowledge, only three previous MC studies[17–19] have simultaneously included magnetic and chemical order-disorder processes in alloys. These studies were concerned with bcc Fe-Al alloys in which only one species is magnetic and all magnetic bonds are ferromagnetic ($J_{\mathrm{FeFe}}>0$). Ours is the first such study in which there are two magnetic species and the possibility of frustration. However, we do not go beyond NN-only chemical interactions nor do we treat entire regions in composition of the phase diagram as in previous studies. Instead, we mainly aim to illustrate both the necessity for taking magnetic and chemical interactions into account simultaneously and the most interesting features that arise. With Fe-Ni, except in limited regions of the phase diagram, one must allow coexisting bcc and fcc phases which greatly complicates true phase diagram calculations at arbitrary compositions.

II. MC METHODS

As is always the case in such calculations,[20] we disallow the phonon degrees of freedom and ignore thermal expansion and elastic strain effects, etc. We also disallow all types of lattice defects such as vacancies, interstitials, intergrain boundaries, magnetic domain walls, etc. We take only the chemical and magnetic (i.e., atomic and spin configuration) disorders into account and conveniently model both using Ising model statistics by the usual MC methods.

We have used lattice sizes, in units of the fcc conventional unit-cell edge length, of $10\times10\times10$, $15\times15\times15$, and $20\times20\times20$ (corresponding to 4000, 13 500, and 32 000 atoms, respectively), with periodic boundary conditions. We find that the lattice size does not affect the reported calculated properties for these sizes.

Three types of simulations were performed for each alloy: (1) magnetic-only excitations allowed with a set predetermined chemical order, (2) chemical-only processes considered with magnetic interactions ignored, and (3) chemical and magnetic excitations allowed simultaneously.

For case (1), the usual metropolis single-flip algorithm was applied as described in detail elsewhere.[14] Here, the Hamiltonian is

$$H=-\sum_{i,j} J_{ij}(\mu_i\mu_j/4\mu_B^2)\sigma_i\sigma_j\,, \tag{1}$$

where the sum is over all NN pairs, μ_i is the atomic moment at site i, μ_B is the Bohr magneton, J_{ij} is either J_{NiNi}, J_{FeNi} or J_{FeFe} depending on i and j, and σ_i is the usual Ising variable (or spin) equal to ±1.

For case (2), rather than work in the usual grand-canonical ensemble where the composition is controlled by a chemical potential,[20] we work directly in the canonical ensemble with fixed composition and use the following algorithm rather than map onto the equivalent spin system: two sites are selected at random and the atoms at these site are interchanged if they are of different species and the MC condition is satisfied. The same final configurations were found if the two sites were imposed to be NN sites however equilibration times were much longer. As in the magnetic calculation, we avoid the problem of domain walls by starting with a perfectly ordered state at $T\approx0$ K and moving up in temperature with small enough steps, using the previous equilibrium state as the new initial state.

For case (3), the same strategy for avoiding domain walls is used except that the system is spin equilibrated at the new temperature before the MC algorithm that combines both chemical and magnetic equilibration is applied. The latter algorithm consists of picking two atoms of different species at random. One also chooses one of the following three options at random: (i) the spins of the two atoms are not changed, (ii) the spin of one atom is flipped, (iii) both spins are flipped. One then exchanges the two atoms (preserving their new spin orientations) if the MC condition with the chosen spin option is satisfied. This algorithm again allows us to work at a constant chosen composition.

III. RESULTS

Each alloy of interest has a single true equilibrium magnetic ordering temperature (or Curie point), T_C(equil), and a single true equilibrium chemical (or atomic) ordering temperature, T_a(equil). At and above T_C(equil), the alloy can have long-range chemical order [if T_C(equil)$<T_a$(equil)] or short-range chemical order only [if T_C(equil)$>T_a$(equil)]. Similarly, at and above T_a(equil), the alloy can have long- or short-range magnetic order. In addition, magnetic ordering temperatures of nonequilibrium (metastable) states can be measured. For example, the alloy can be quenched from the melt into an almost perfectly random chemical state and then its magnetic transition, T_C(random), is measured in a time too short to allow significant chemical ordering. Similarly, when T_C(equil)$\ll T_a$(equil), the magnetic ordering temperature of the perfectly chemically ordered state, T_C(ordered), is approximately given by T_C(equil).

A. Magnetic interactions only

In this section, we simulate the magnetic properties of Fe_3Ni, FeNi, and $FeNi_3$ alloys that are either in a perfectly ordered chemical state or in a perfectly random chemical state. This shows conclusively the large effect that the degree of chemical order is predicted to have on the magnetic properties. The NN magnetic exchange constants [J_{ij}'s in Eq. (1)] that we use are those obtained from a detailed comparison between simulations and experiments on quenched chemically random state alloys in the entire accessible composition range:[14] $J_{\mathrm{NiNi}}=700$ K, $J_{\mathrm{FeNi}}=355$ K, and $J_{\mathrm{FeFe}}=-25$ K. These correspond to magnetic bond energies ($|J_{ij}\mu_i\mu_j/4\mu_B^2|$) of 65, 150, and 50 K, respectively.

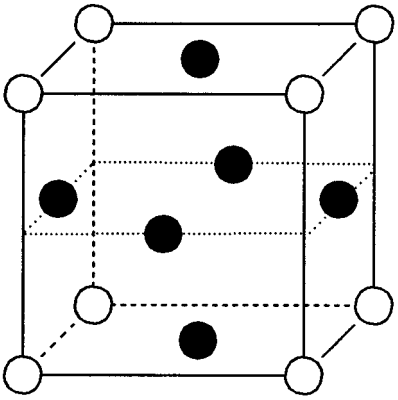

FIG. 1. Conventional unit cell of chemically ordered $FeNi_3$ (or Fe_3Ni) with filled circles representing Ni (or Fe) atoms and open circles representing Fe (or Ni) atoms.

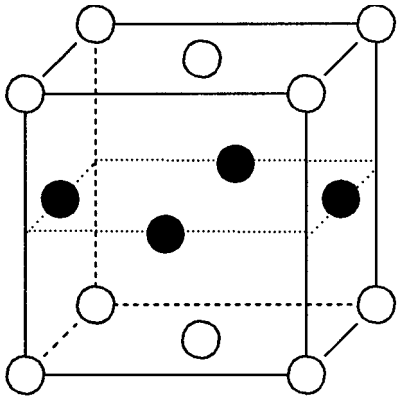

FIG. 3. Conventional unit cell of chemically ordered FeNi with filled circles representing Ni (or Fe) atoms and open circles representing Fe (or Ni) atoms.

The crystal structure of the chemically ordered state of $FeNi_3$ is shown on the conventional fcc cell in Fig. 1. The results for $FeNi_3$ are illustrated in Fig. 2 where the spontaneous average moment per atom μ and the zero-field average magnetic energy per atom E_{magn}, are shown as functions of temperature for the chemically ordered and random states. Here $\mu(T)$ shows the usual finite-size effects just above T_C, however, $E_{\text{magn}}(T)$ does not have noticeable finite-size effects and its tails above T_C are due to true magnetic short-range order. The magnetic ordering temperatures are equally well estimated from the $\mu(T)$ curves or from the inflection points in the $E_{\text{magn}}(T)$ curves. These estimates give sufficiently small errors of approximately 5–10 K (~1–2 %) such that it was not necessary to use the cumulant intersection method to locate T_C.

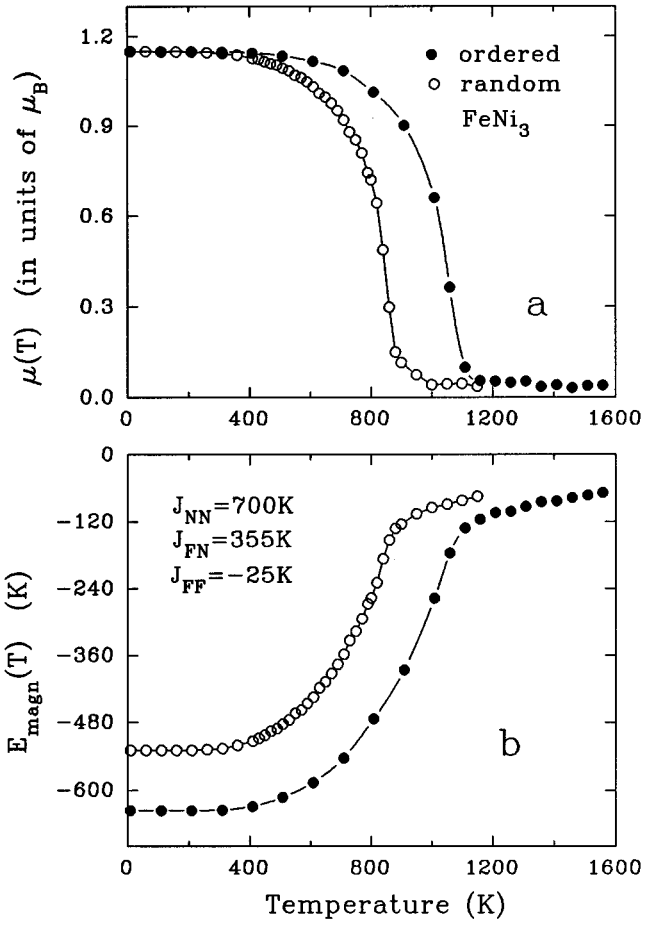

FIG. 2. MC simulated magnetic properties of $FeNi_3$ allowing only the magnetic degrees of freedom and assuming either perfect chemical randomness (open circles) or perfect chemical order (filled circles): (a) spontaneous average moment per atom versus temperature, (b) average magnetic energy per atom versus temperature.

The simulation values for T_C(ordered) and T_C(random) in $FeNi_3$ are 1180 and 870 K, respectively. This compares favorably with the best experimental values of[21] 940 and[22] 850 K, respectively. The experimental value for T_C(ordered) is an underestimate related to the fact that the measured T_a in $FeNi_3$ is[23] 770 K, significantly below T_C(ordered) at temperatures where diffusion is relatively fast for the magnetization measurements used. Our simulation therefore predicts the true value of T_C(ordered), to be compared with an eventual value from a sufficiently fast measurement. Even an instantaneous measurement of T_C by heating would also represent an underestimate, however, because the perfectly chemically ordered initial state cannot be prepared and is ultimately limited by the required annealing times at low temperatures.

Finally, note that the simulated saturation moments per atom of both chemically ordered and random $FeNi_3$ are exactly the same and equal to the measured value of $1.15\mu_B$. This value corresponds to all Fe and Ni moments being ferromagnetically aligned (i.e., $0.25\times2.8\mu_B+0.75\times0.6\mu_B$). The difference in ground-state magnetic energy per atom of the chemically ordered and random alloys is $E_{\text{magn}}(\text{ordered};T=0)-E_{\text{magn}}(\text{random};T=0)=-107$ K.

The crystal structure of the chemically ordered state of FeNi is shown on the conventional fcc cell in Fig. 3. The results for FeNi are illustrated in Fig. 4. Here, the simulation values for T_C(ordered) and T_C(random) are 1020 and 820 K, respectively. The latter compares well with the measured value of[22] 785 K. Because of the low chemical ordering temperature of only[24] 593 K for this alloy, the measured T_C(ordered) for FeNi should be considered an underestimate

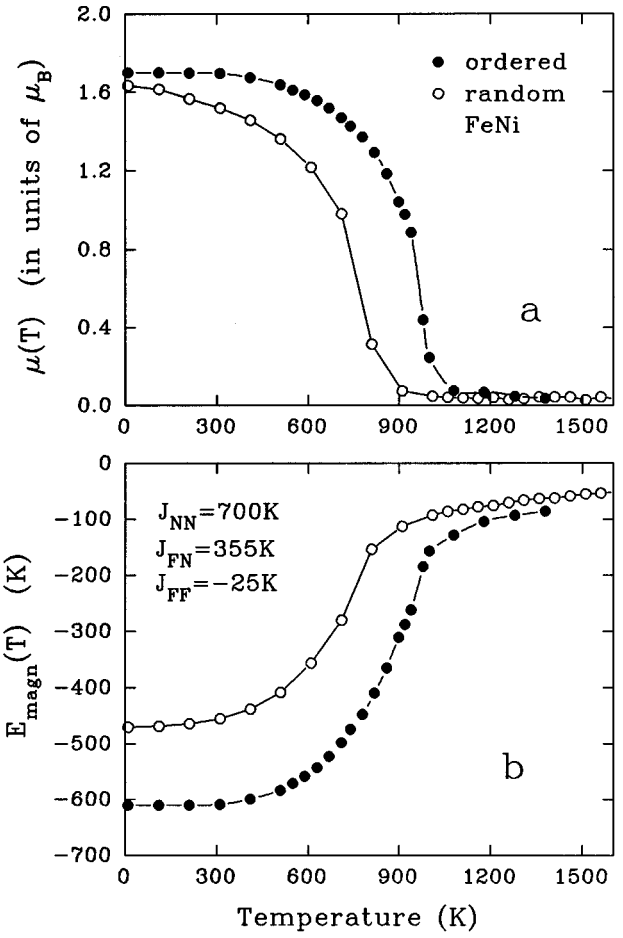

FIG. 4. MC simulated magnetic properties of FeNi allowing only the magnetic degrees of freedom and assuming either perfect chemical randomness (open circles) or perfect chemical order (filled circles): (a) spontaneous average moment per atom versus temperature, (b) average magnetic energy per atom versus temperature.

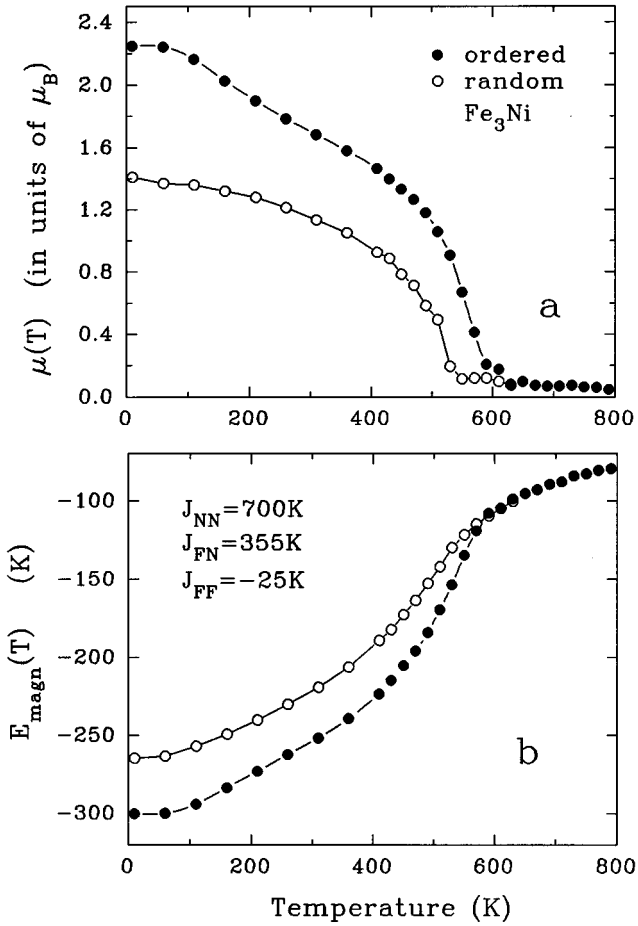

FIG. 5. MC simulated magnetic properties of Fe_3Ni allowing only the magnetic degrees of freedom and assuming either perfect chemical randomness (open circles) or perfect chemical order (filled circles): (a) spontaneous average moment per atom versus temperature, (b) average magnetic energy per atom versus temperature.

and is[25] 840 K. Indeed, an FeNi sample with significant chemical order has, to our knowledge, never been synthetically produced by simple annealing. Particle irradiation is required in the laboratory and most of what is known about chemically ordered FeNi comes from iron meteorite studies where it is called tetrataenite.[3]

For FeNi, the chemically ordered state again has a higher T_C but the spontaneous magnetic moment curves for the ordered and random phases now have two notable differences that were not exhibited in $FeNi_3$. First, the saturation moments per atom are significantly different. That of the chemically ordered phase is $1.70\mu_B$ corresponding as expected to complete ferromagnetic alignment $(0.5\times 2.8\mu_B + 0.5 \times 0.6\mu_B)$ whereas that of the chemically random phase is $1.68\mu_B$ corresponding to 0.71% of the Fe moments being in local environments such that they are antiferromagnetically aligned with the sample magnetization. Secondly, the $\mu(T)$ curve for the chemically random phase is flattened in comparison with that of the chemically ordered phase. This is a common effect of disorder in magnetic systems and arises from the fact that there are many local environments in which the moments can be thermally excited even at the lower temperatures compared to T_C.

The crystal structure of the chemically ordered state of Fe_3Ni is taken to be the same as that of $FeNi_3$ (Fig. 1) with Fe and Ni atoms interchanged. Chemically ordered Fe_3Ni has never been synthesized or conclusively observed in nature. At this composition, synthetic alloys are usually bcc since the bcc/fcc instability occurs at ~30 at. % Ni at RT. Nonetheless, there have been suggestions[3] that the occurrence of chemically ordered Fe_3Ni could resolve various difficulties related to the metallurgy of both particle-irradiated synthetic Fe-Ni alloys and meteoritic Fe-Ni alloys. It therefore seems worthwhile to extend our simulations to Fe_3Ni and to consider our results as predictions that cannot yet be compared with sufficiently complete experimental data.

Note that, at this composition, a low-spin fcc state may be more thermodynamically stable than the high-spin fcc state[3,26] that we model for the sake of describing its characteristics. Also, recently,[27] bulk amounts of high-spin fcc phase have been produced by mechanical alloying, to Fe contents as high as 80 at. % Fe.

The results for Fe_3Ni are illustrated in Fig. 5. Here again, the chemically ordered state has a higher T_C than the chemically random state, 580 versus 520 K, respectively. The $\mu(T)$ curves themselves, however, for the chemically ordered and

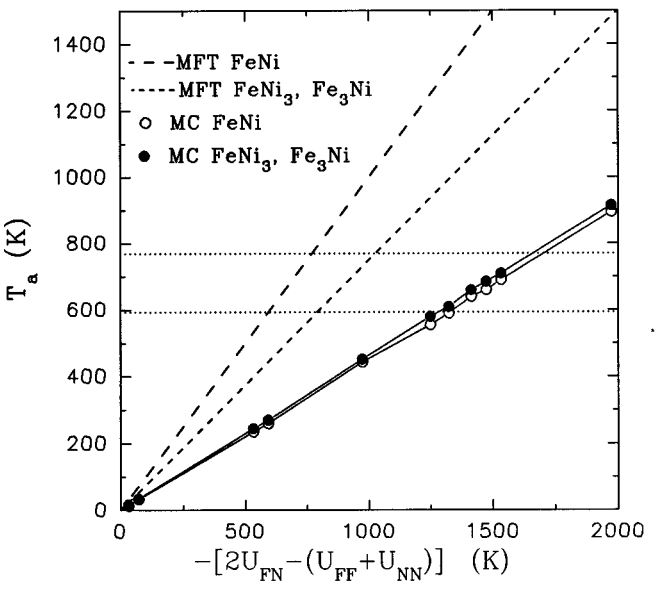

FIG. 6. Chemical (or atomic) order-disorder transition temperature T_a versus minus the bond energy parameter $U \equiv 2U_{\mathrm{FeNi}}\text{-}U_{\mathrm{FeFe}}\text{-}U_{\mathrm{NiNi}}$ calculated: by MFT for FeNi (dashed line), by MFT for $FeNi_3$ and Fe_3Ni (dotted line), by MC for FeNi (open circles), by MC for $FeNi_3$ and Fe_3Ni (closed circles). The horizontal lines show the measured T_a values for FeNi (593 K) and $FeNi_3$ (770 K).

random states are much more different for Fe_3Ni than they are for FeNi or $FeNi_3$. The saturation moment per atom for chemically ordered Fe_3Ni is $2.25\mu_B$, corresponding to all Fe and Ni moments being ferromagnetically aligned, whereas, for disordered Fe_3Ni it is only $1.41\mu_B$, corresponding to 20.0% of the Fe moments being antiferromagnetically aligned to the bulk magnetization. Figure 5 also shows that the $\mu(T)$ curve for chemically ordered Fe_3Ni has some structure in the $T=100-400$ K range. This arises from the very different magnetic coupling strengths of Fe and Ni in this structure.

B. Chemical interactions only

We model the chemical binding forces by NN-only bonds, U_{NiNi}, U_{NiFe}, and U_{FeFe}, that depend only on the identities of the interacting NN atoms. Some justification for this is given by electronic-structure calculations.[28] The Ni-Ni bond is taken to be that, $U_{\mathrm{NiNi}}=-8590$ K, which corresponds to the measured cohesive energy of fcc nickel,[29] assuming that the chemical bond energy is the dominant contribution. The Fe-Fe bond is taken to correspond to the cohesive energy of high-spin fcc iron, obtained by extrapolation from the measured cohesive energies[29] of fcc copper, fcc nickel, and hcp cobalt: $U_{\mathrm{FeFe}}=-8400$ K. This leaves U_{NiFe} which is taken to give the best agreement between the measured T_a(equil) values for FeNi and $FeNi_3$ and the MC values, T_a(chem), including only chemical interactions (see below): $U_{\mathrm{NiFe}}=-9200$ K.

Many other values of the bond energies were also used in order to evaluate how they determine the value of T_a(chem), allowing chemical interactions only. Typical results are shown in Fig. 6 where it is seen that, just as in MFT, T_a(chem) is proportional to the particular combination $U \equiv 2U_{\mathrm{NiFe}}\text{-}U_{\mathrm{FeFe}}\text{-}U_{\mathrm{NiNi}}$, irrespective of the individual values used. Also, just as in MFT, the T_a(chem) for Fe_3Ni is the same, for a given value of U, as that for $FeNi_3$. The proportionality constants, however, are different for MFT and MC simulations: As usual, MFT overestimates the ordering temperatures because it disallows fluctuations.

Another interesting difference between the MFT and MC predictions seen in Fig. 6 is that MFT has the T_a(chem) of FeNi being larger than that of $FeNi_3$ whereas MC has the T_a(chem) of FeNi being smaller than that of $FeNi_3$, in better agreement with the measured T_a(equil) values. Also, MFT predicts a second-order transition for FeNi and first-order transitions for Fe_3Ni and $FeNi_3$, whereas the transitions obtained by MC appear similar in character for all three alloys (see below) and are probably first order.

In describing the degree of chemical order and the chemical order-disorder transition, we define two quantities: the long-range order parameter (LROP) p and the short-range order parameter (SROP) r. Both have the value 1 in the perfectly ordered state and the value 0 in the perfectly random state. The lattices of the ordered binary alloys are divided into sublattices A and B; the two sublattices that receive Fe and Ni atoms, respectively, in the perfectly ordered states.

In the FeNi system, p is defined by

$$N_{\mathrm{Fe},A}=N(1+p)/2, \tag{2}$$

where $N_{\mathrm{Fe},A}$ is the number of Fe atoms on sublattice A and N is the total number of Fe atoms. In this system, the SROP is defined by

$$r=q-3, \tag{3}$$

where q is the average number of NN Fe-Ni bonds per atom. Here, $q=4$ for perfectly ordered FeNi and $q=3$ for perfectly random FeNi (Fig. 3). In other words, r measures the preference for Fe-Ni bonds that drives the ordering process. It can be nonzero above T_a where the LROP is zero.

Similarly, in the $FeNi_3$ system, the LROP is defined by

$$N_{\mathrm{Fe},A}=N(1+3p)/4 \tag{4}$$

and the SROP is given by

$$r=(4q-9)/3, \tag{5}$$

where $q=3$ for perfectly ordered $FeNi_3$ and $q=9/4$ for perfectly random $FeNi_3$. The same holds for Fe_3Ni, with Fe and Ni interchanged.

Figure 7 shows the LROP, the SROP, and the chemical bond energy per atom E_{chem}, as functions of temperature for $FeNi_3$. Figures 8 and 9 show the same properties for FeNi and Fe_3Ni, respectively. In all three cases both the SROP and E_{chem} show significant short-range order far above T_a. This, with the results of the previous section, shows that chemical order can significantly affect the magnetic properties even when T_C is much larger than T_a. It also suggests, contrary to what is often assumed, that rapid quenching from the melt to a perfectly random state is impossible.

Finally, Fig. 6 shows that it is impossible to match the measured T_a(equil) values for FeNi and $FeNi_3$ (593 and 770 K, respectively) with the MC T_a(chem) values using a single

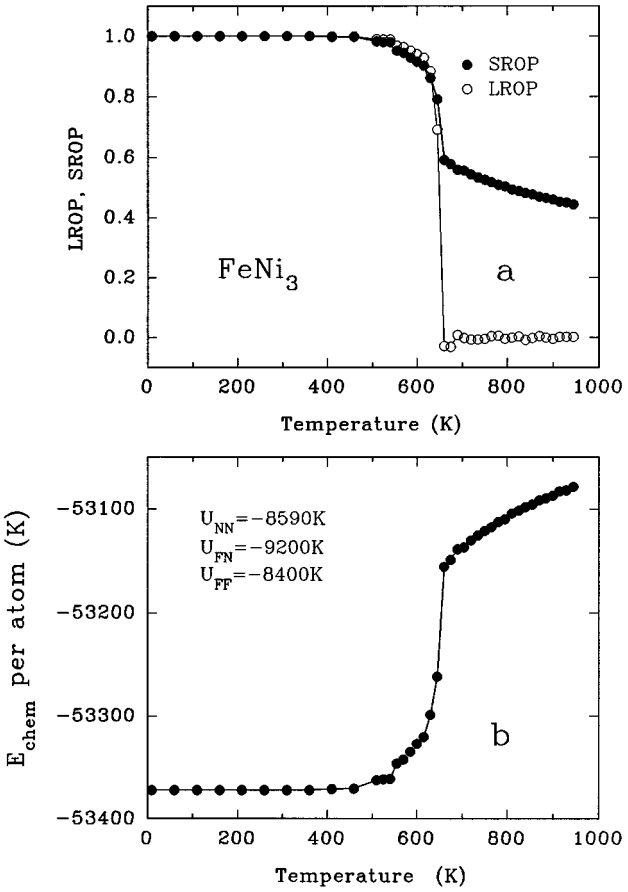

FIG. 7. MC simulated crystal chemical properties of $FeNi_3$ allowing only the chemical (i.e., atomic position exchange) degree of freedom and neglecting the magnetic interactions: (a) the LROP, p (open circles) and SROP, r (filled circles) versus temperature, (b) the average chemical bond energy per atom versus temperature.

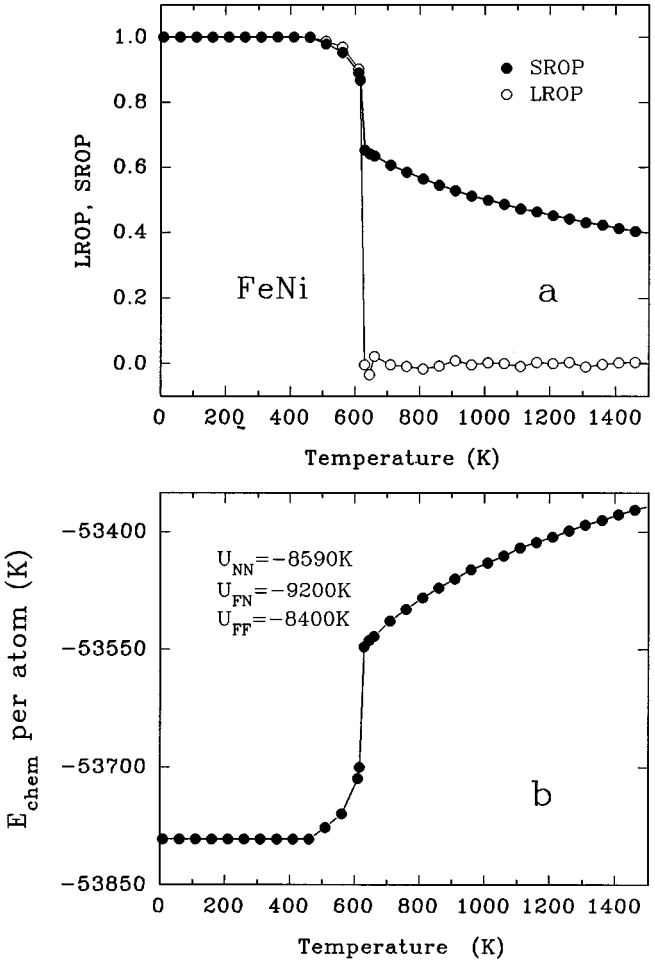

FIG. 8. MC simulated crystal chemical properties of FeNi allowing only the chemical (i.e., atomic position exchange) degree of freedom and neglecting the magnetic interactions: (a) the LROP, p (open circles) and SROP, r (filled circles) versus temperature, (b) the average chemical bond energy per atom versus temperature.

value of U. Fair agreement occurs at $U=-1410$ K and this was used to evaluate U_{FeNi} but it is not good agreement (Fig. 6). This is not surprising given the simplicity of the model: NN-only two-body interactions, etc. Nonetheless, it is interesting to explore the extent to which such matching is possible simply by simultaneously allowing the chemical and magnetic degrees of freedom. It is equally interesting to see the extent to which each of the isolated behaviors is changed by the coexistence.

C. Simultaneous magnetic and chemical interactions

In Sec. III A, we calculated T_C(ordered) and T_C(random) by allowing only the magnetic interactions and by assuming either perfect chemical order or perfect chemical randomness, respectively. As mentioned above, it is possible to perform nonequilibrium measurements of T_C(ordered) and T_C(random) because the magnetic equilibration time is much shorter than the chemical equilibration time. Of course, with a sufficiently slow measurement, what is measured is T_C(equil). In Sec. III B, we calculated T_a(chem) by allowing only the chemical interactions. What is measured, however, is always T_a(equil). In this section, we calculate T_a(equil) and T_C(equil) by assuming that the chemical and magnetic interactions are the dominant interactions.

Clearly, T_C(equil) will be between T_C(random) and T_C(ordered), depending on the degree of chemical long- or short-range order at T_C(equil). In addition, one of the main results of the present paper, is that T_a(equil) is significantly different from T_a(chem), even if T_a(equil)$>T_C$(equil), and is only equal to T_a(chem) if T_a(equil)$\gg T_C$(equil) such that magnetic short-range order is negligible at T_a(equil).

The results for $FeNi_3$, taking the same magnetic and chemical interaction parameters as before, are shown in Fig. 10. Here, the average spin per atom, $\langle S\rangle$, is shown instead of the average moment per atom $[\langle S\rangle=\mu(T)/2\mu_B]$, on the same scale as the chemical long-range and short-range order parameters. The chemical and magnetic contributions to the total average energy per atom and the latter total energy are also shown. In comparing to Figs. 2 and 7, for $FeNi_3$, we note that T_C(equil) is larger than T_C(random) and smaller than T_C(ordered) because of the chemical short-range order. We also note that T_a(equil) is larger than T_a(chem) because of the presence of magnetic order, and that an abrupt step of magnitude $0.04\mu_B$ per atom occurs in the equilibrium spontaneous magnetization at T_a(equil).

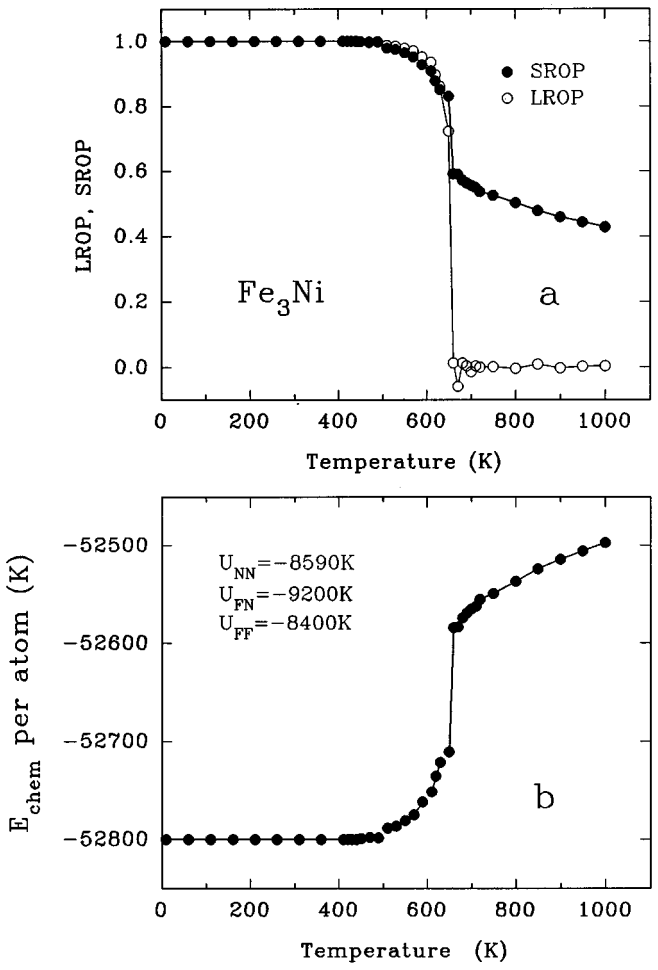

FIG. 9. MC simulated crystal chemical properties of Fe_3Ni allowing only the chemical (i.e., atomic position exchange) degree of freedom and neglecting the magnetic interactions: (a) the LROP, p (open circles) and SROP, r (filled circles) versus temperature, (b) the average chemical bond energy per atom versus temperature.

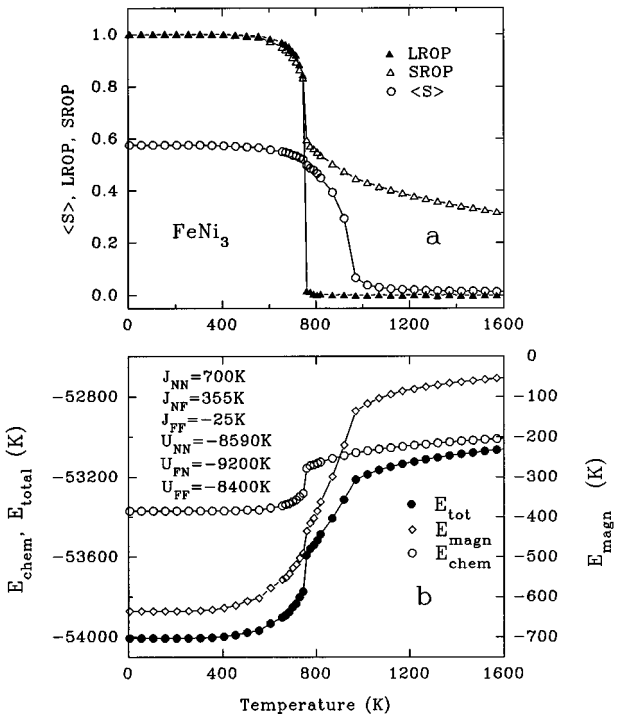

FIG. 10. MC simulated crystal chemical and magnetic equilibrium properties of $FeNi_3$ allowing both chemical and magnetic degrees of freedom simultaneously: (a) chemical LROP (filled triangles), chemical SROP (open triangles), and average spin per atom $\langle S\rangle$ (open circles), as functions of temperature; (b) chemical energy per atom (open circles, left scale), magnetic energy per atom (open diamonds, right scale), and total energy per atom (filled circles, left scale), as functions of temperature.

Similar results for FeNi are shown in Fig. 11. An abrupt step of magnitude $0.1\mu_B$ per atom occurs in the equilibrium spontaneous magnetization at the presumably first-order chemical ordering transition. The chemical and magnetic ordering temperatures are affected by the combined magnetic and chemical interactions in a qualitatively similar way as in $FeNi_3$.

The results for Fe_3Ni are shown in Fig. 12. Contrary to $FeNi_3$ and FeNi, Fe_3Ni has $T_C(\text{equil})<T_a(\text{equil})$. In comparing Fig. 12 to Fig. 5, one notes that the spontaneous average moment per atom for the case of combined interactions is the same within error as for the case of magnetic only interactions with fixed perfect chemical order. This is because, even for temperatures up to T_C(equil) in the case of combined interactions, the chemical LROP is not significantly lower than 1. In particular, the same structure at $T=100-400$ K in $\langle S\rangle$ versus T [or $\mu(T)$] is present and $T_C(\text{equil})=T_C(\text{ordered})$, within error. The chemical ordering temperature in the case with combined interactions (Fig. 12) is also the same within error as in the case of chemical only interactions (Fig. 9). However, we have found that with different choices of the NN chemical bond parameters that give comparable values of T_a(equil) it is usual for T_a(equil) to be larger than T_a(chem), by typically 30 K or so. This occurs despite the fact that $T_C(\text{equil})<T_a(\text{equil})$ because of magnetic short-range order above T_C(equil). Most interestingly, whereas with chemical only interactions $FeNi_3$ and Fe_3Ni had the same chemical ordering temperatures (Fig. 6), with combined chemical and magnetic interactions they have significantly different T_a(equil) values.

The above results concerning the various ordering temperatures are given more quantitatively in Tables I and II. We see that (Table I), in the cases of $FeNi_3$ and FeNi where $T_C(\text{equil})>T_a(\text{equil})$, the chemical ordering temperatures are increased by 100 K, relative to chemical only interactions. Regarding the magnetic ordering temperatures (Table II), recall (Sec. III A) that the measured values are estimates, given the kinetics involved and the nonzero and finite measurement times. For all three alloys, $T_C(\text{random})\leqslant T_C(\text{equil})\leqslant T_C(\text{ordered})$, as expected. All three alloys have $T_C(\text{random})<T_C(\text{ordered})$ and the difference between T_C(random) and T_C(ordered) decreases as Fe content increases. The relationship between the latter difference and Fe content is expected to be complicated because the degree of magnetic frustration in the disordered alloys increases with Fe content.

It is also of interest to examine how long- and short-range magnetic order affect chemical short-range order above T_a(equil). This is shown in Figs. 13 and 14 where the chemical SROP's are plotted versus T/T_a for chemical-only and

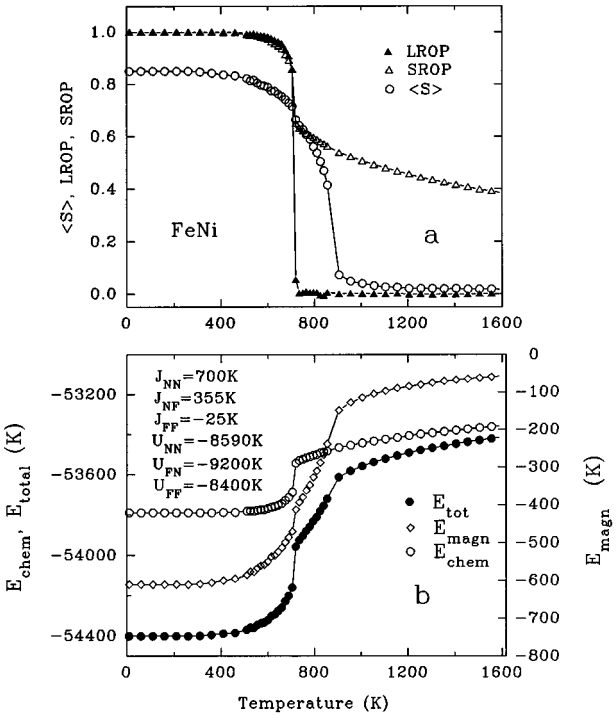

FIG. 11. MC simulated crystal chemical and magnetic equilibrium properties of FeNi allowing both chemical and magnetic degrees of freedom simultaneously. The symbols have the same meanings as in Fig. 10.

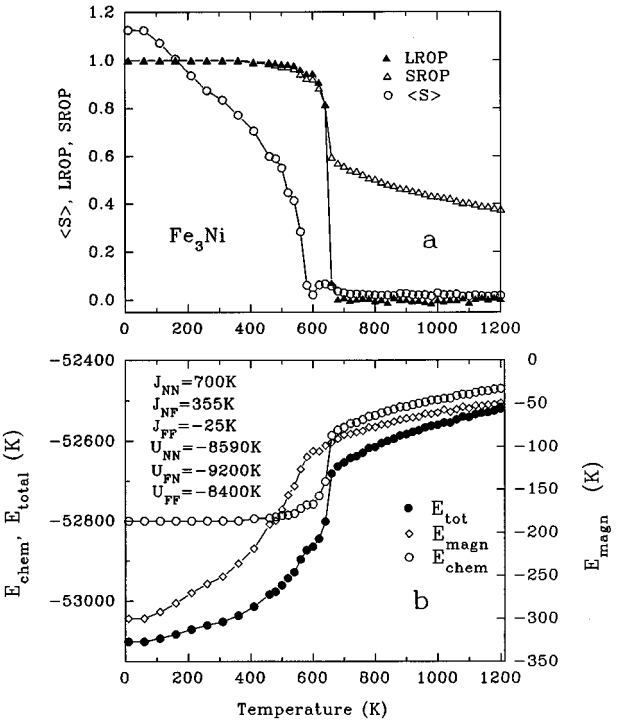

FIG. 12. MC simulated crystal chemical and magnetic equilibrium properties of Fe_3Ni allowing both chemical and magnetic degrees of freedom simultaneously. The symbols have the same meanings as in Fig. 10.

TABLE I. MC and measured chemical ordering temperatures in K.

	MC		Measured
Alloy	T_a(chem)	T_a(equil)	T_a(equil)
$FeNi_3$	660	760	770
FeNi	620	720	593
Fe_3Ni	660	660	

combined chemical and magnetic interactions, for $FeNi_3$ and FeNi, respectively. For both alloys, the value of T_C(equil)/T_a(equil) on the T/T_a axis is shown by a vertical dashed line. The corresponding chemical SROP's as functions of T/T_a for Fe_3Ni, which has T_C(equil)$<T_a$(equil), are equal within error (± 0.003) at all $T/T_a>1$.

Figures 13 and 14 show that, in cases where T_C(equil)$>T_a$(equil), the magnetically induced contributions to the chemical short-range order are largest at temperatures below T_C(equil) and decrease monotonically as $T/T_a \rightarrow T_C$(equil)/T_a(equil) but remain significant far above T_C(equil)/T_a(equil), as they continue to decrease as temperature is increased. Below T_C(equil) the magnetically induced increase in chemical short-range order is about 10% whereas just above T_C(equil) it is about 1–2 %. Therefore, both magnetic long-range order and magnetic short-range order affect chemical short-range order above T_a.

D. General predictions with combined chemical and magnetic interactions

We now diverge a little from the specific cases of $FeNi_3$, FeNi, and Fe_3Ni alloys in order to consider some interesting additional predicted phenomena that arise when chemical

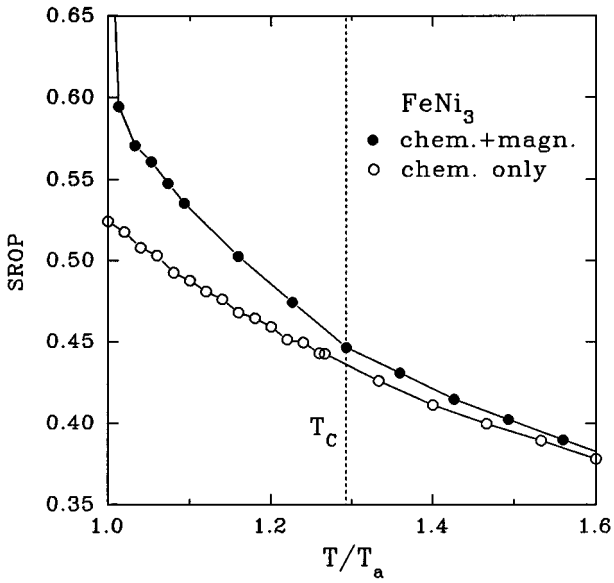

FIG. 13. MC simulated equilibrium chemical SROP versus T/T_a(equil) for $FeNi_3$ calculated either with chemical interactions only (open circles) or with both chemical and magnetic interactions (filled circles). The position of T_C(equil) is shown by a vertical dashed line.

TABLE II. MC and measured magnetic ordering temperatures in K.

	MC			Measured	
Alloy	T_C(random)	T_C(ordered)	T_C(equil)	T_C(random)	T_C(ordered)
$FeNi_3$	870	1180	970	850	940
FeNi	820	1020	910	785	840
Fe_3Ni	520	580	580		

and magnetic interactions act simultaneously. In particular, we examine how the general behavior depicted in Fig. 6 is affected by including the magnetic interactions.

Typical results are shown in Fig. 15. We find that, for a given set of magnetic exchange parameters, the differential bond energy parameter $U \equiv 2U_{\mathrm{FeNi}}\text{-}U_{\mathrm{FeFe}}\text{-}U_{\mathrm{NiNi}}$ is again a valid parameter in that, for each alloy, T_a(equil) is a function only of U, not of the particular values of U_{FeNi}, U_{FeFe}, and U_{NiNi}. By comparing with Fig. 6, we note several new features in Fig. 15: $FeNi_3$ and Fe_3Ni have different chemical ordering temperatures and the T_a versus U curves are no longer linear and no longer intersect the origin. Also, the T_a(equil) versus U curves (Fig. 15) approach the MC T_a(chem) versus U curves (Fig. 6) as U increases. The latter behavior is expected because as U increases, for fixed magnetic exchange parameters, the chemical component of the change in energy per exchange in the atomic positions of an Fe-Ni pair becomes much larger than the magnetic component.

The special case of Fe_3Ni stoichiometry is discussed below. The fact that, for $FeNi_3$ and FeNi stoichiometries, the T_a(equil) versus U curves intersect the $U=0$ axis at positive T_a(equil) values means that the magnetic interactions induce chemical order in these systems, that have no chemical bond energy preference for chemical order.

This is shown for $FeNi_3$ stoichiometry in Fig. 16 where, although $U=0$, T_a(equil)$=140$ K. The chemical order-disorder transition does not cause a break in the magnetization because at temperatures well below T_C(equil) [or T_C(random) or T_C(ordered)] the chemically random and ordered states have the same (saturation) moment per atom. By comparison, the break seen in Fig. 10 (or Fig. 11) arises from the combined facts that T_a(equil)$\sim T_C$(equil) and T_C(random)$\neq T_C$(ordered), such that, as the temperature is increased through T_a(equil), the magnetization (or $\langle S \rangle$) at T_a(equil) goes from one corresponding to a large T_C [$\sim T_C$(ordered)] to one corresponding to a smaller T_C [$\sim T_C$(random)].

Also, a $U=0$ system with chemical only interactions has chemical long- and short-range order parameters of zero at all nonzero temperatures, however, Fig. 16 shows that our $U=0$ $FeNi_3$ system with magnetic interactions has significant chemical short-range order up to T_C(equil) and nonzero values of the chemical SROP even above T_C(equil). Here, the chemical SROP is clearly correlated to $\langle S \rangle$, dropping

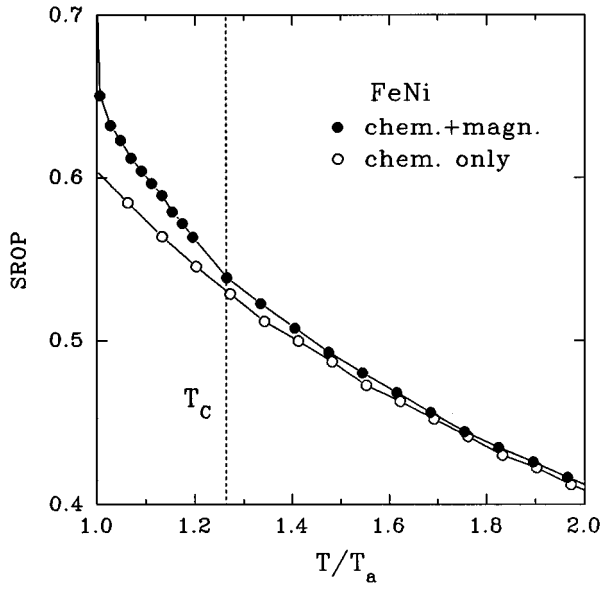

FIG. 14. MC simulated equilibrium chemical SROP versus T/T_a(equil) for FeNi calculated either with chemical interactions only (open circles) or with both chemical and magnetic interactions (filled circles). The position of T_C(equil) is shown by a vertical dashed line.

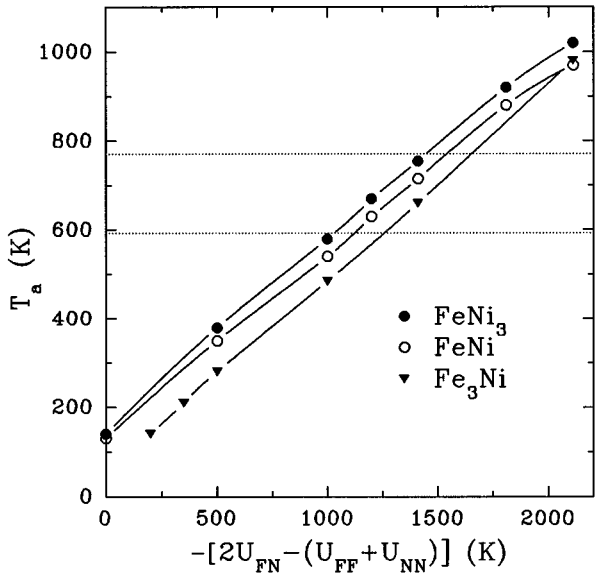

FIG. 15. Chemical (or atomic) order-disorder transition temperature T_a versus minus the bond energy parameter $U \equiv 2U_{\mathrm{FeNi}}\text{-}U_{\mathrm{FeFe}}\text{-}U_{\mathrm{NiNi}}$ obtained from MC simulations that combine the chemical and magnetic interactions (with $J_{\mathrm{NiNi}}=700$ K, $J_{\mathrm{FeNi}}=355$ K, and $J_{\mathrm{FeFe}}=-25$ K) for $FeNi_3$ (filled circles), FeNi (open circles), and Fe_3Ni (filled triangles). The horizontal lines show the measured T_a values for FeNi (593 K) and $FeNi_3$ (770 K).

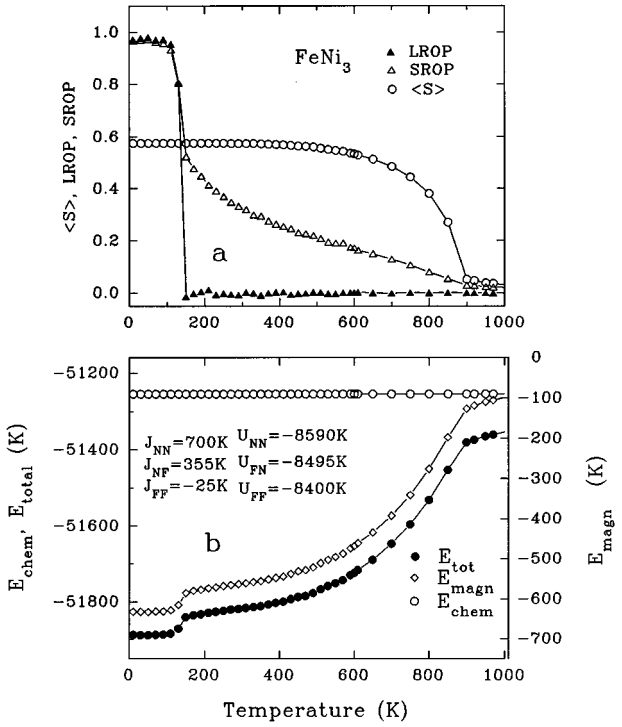

FIG. 16. MC simulated crystal chemical and magnetic equilibrium properties, allowing both chemical and magnetic degrees of freedom simultaneously, for $FeNi_3$ with U_{FeNi} adjusted such that $U=0$: (a) chemical LROP (filled triangles), chemical SROP (open triangles), and average spin per atom $\langle S\rangle$ (open circles), as functions of temperature; (b) chemical energy per atom (open circles, left scale), magnetic energy per atom (open diamonds, right scale), and total energy per atom (filled circles, left scale), as functions of temperature.

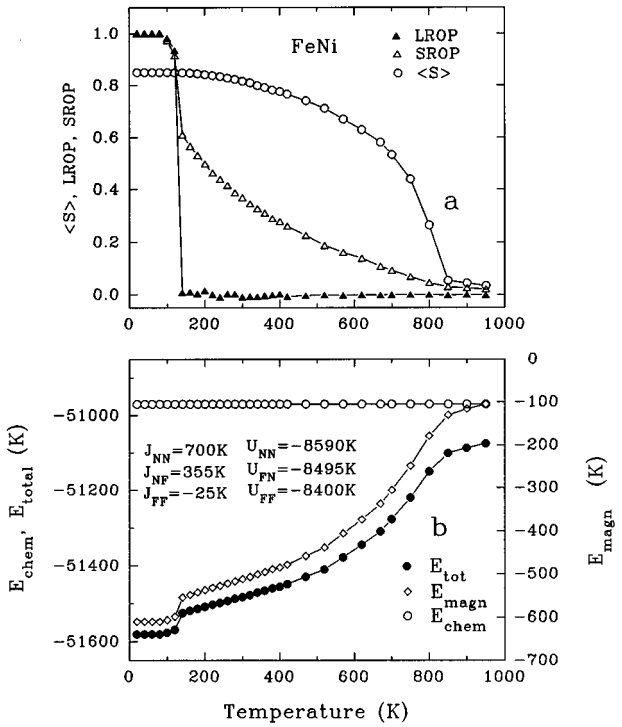

FIG. 17. MC simulated crystal chemical and magnetic equilibrium properties, allowing both chemical and magnetic degrees of freedom simultaneously, for FeNi with U_{FeNi} adjusted such that $U=0$. The symbols have the same meanings as in Fig. 16.

more rapidly when $\langle S\rangle$ drops as T_C(equil) is approached. As with $U\neq 0$ systems (Figs. 13 and 14), the chemical SROP is nonzero above T_C(equil) because of magnetic short-range order, although the simulated behavior is somewhat imprecise here due to finite-size effects that cause $|\langle S\rangle|$ to be nonzero above T_C(equil).

Figure 17 shows an analogous situation for the FeNi $U=0$ case where a T_a(equil)=130 K is induced by the magnetism. In addition, we have found that it is possible to induce a T_a(equil)>0 and significant chemical short-range order to high temperatures up to $T\sim T_C$(equil) in systems that, from a chemical-only perspective, would phase separate ($U>0$). This suggests that real systems could be found that are miscible below a magnetic ordering temperature and phase separate above the magnetic ordering temperature.

Finally, we describe the more complicated case of Fe_3Ni stoichiometry with $U\simeq 0$. Here additional interesting features are expected because, due to magnetic frustration, the saturation moments per atom are very different for the chemically ordered and disordered states (Fig. 5). Indeed, at $U=0$, the chemically ordered state is not stabilized by the magnetism at any temperature, such that T_a is not defined. At $T=0$ K, a completely segregated (Fe and Ni phase separated state) leads to lower total energy than either a chemically ordered or disordered state with equilibrated spin structure. The ground state seems to be a complicated (possibly compositionally modulated or banded) segregated state. This also holds for small negative U, up to $U\simeq -50$ K where segregated and ordered states have about the same energies at $T=0$ K. At $U=-100$ K, a stable chemically ordered ground state is found but the higher temperature behavior is ambiguous with T_a being difficult to locate. Normal behavior, such as that depicted in Figs. 16 and 17, is recovered at $U=-200$ K, which is the last point shown on the graph (Fig. 15).

Although more work is needed, that is beyond the scope of the present paper, the case of Fe_3Ni stoichiometry shows that magnetism can induce phase separation in a system whose chemical only interactions would give rise to miscibility. Even if they occur at low temperatures, such phenomena could potentially be observed in slowly cooled meteorites (e.g., 1 K/Ma) or by particle irradiation treatments at low temperatures.[3]

IV. CONCLUSIONS

We have shown that in $FeNi_3$, FeNi, and Fe_3Ni alloys, with typical values of the interaction parameters that give agreement with measured properties, it is necessary to include both chemical and magnetic degrees of freedom in simulating the equilibrium properties because, not only does the degree of chemical order affect the magnetism (i.e., saturation moments, Curie points, degree of magnetic order, etc.), but the presence of magnetic interactions also significantly affects the crystal chemical properties (i.e., chemical ordering temperatures, chemical long- and short-range order parameters, etc.).

Just as chemical order effects on the magnetism can extend to temperatures much greater than the chemical order-disorder transition temperature because of chemical short-range order, magnetic effects on the chemical ordering process can extend beyond the magnetic ordering temperature because of magnetic short-range order. Above the chemical and magnetic ordering temperatures, the chemical and magnetic interactions continue to be important simultaneously in determining both the chemical and magnetic properties.

What matters is not that the chemical bond energies (U_{ij}) are much larger than the magnetic bond energies ($J_{ij}S_iS_j$) but that the *change* in chemical energy per atom is comparable in magnitude to the change in magnetic energy per atom, on crossing the chemical order-disorder transition. In the Fe-Ni alloys, which are typical magnetic transition-metal compound-forming alloys, the magnetic component to the driving force for chemical order is comparable in magnitude to the chemical bond component.

The results of the present work allow one to make the following suggestions concerning Fe-Ni metallurgy and future work on metallic magnetic alloys in general. In attempting theoretical descriptions of the equilibrium structural phase diagram of Fe-Ni: (1) magnetic interactions must be included, and (2) MFT cannot be used for either the magnetic degrees of freedom (because of magnetic frustration and magnetic short-range order) or the chemical degrees of freedom (because chemical ordering temperatures are over estimated and chemical short-range order is ignored).

The present work shows that when the differential chemical bond parameter U is small (or even positive) the magnetic interactions can dominate the chemical ordering processes. New predicted phenomena include: magnetically induced chemical order, magnetically induced chemical segregation, and magnetically driven miscibility/phase-separation transitions. Often, such phenomena will not be observed simply because the chemical equilibration times are too long at the temperatures where they occur. This can be surmounted experimentally by using low-temperature particle irradiation as a means of achieving equilibrium (e.g., Ref. 3).

Finally, recent progress has been made in including chemical and magnetic interactions by doing electronic-structure calculations to examine chemical short-range order at high temperatures.[30] With such elaborate calculations, it is difficult to include certain important realistic effects such as chemical disorder-induced local lattice deformation, whereas, it would be relatively easy to combine MC simulations such as ours with molecular dynamics to include: local strain, atomic vibrations, and various defects. Nonetheless, *ab initio* electronic-structure calculations are needed to test the degree of validity of the simplifying assumptions used in the more phenomenological simulations, and to supply estimates of the various microscopic parameters that are used. Electronic-structure calculations, when they include realistic features, supply a rigorous footing whereas the simulations can give transparent views of the key driving mechanisms. The two approaches should complement each other.

ACKNOWLEDGMENTS

The Natural Sciences and Engineering Research Council of Canada is gratefully acknowledged for financial support.

*Author to whom correspondence should be addressed. Electronic address: DGR@PHYSICS.UOTTAWA.CA

[1] M. Shiga, in *Materials Science and Technology*, edited by R. W. Cahn, P. Haasen, and E. J. Kramer (VCH, Weinheim, 1994), Vol. 3B, Part II, p. 159; D. G. Rancourt, S. Chehab, and G. Lamarche, J. Magn. Magn. Mater. **78**, 129 (1989); J. Y. Ping, D. G. Rancourt, and R. A. Dunlap, *ibid*. **103**, 285 (1992), and references therein.

[2] K. B. Reuter, D. B. Williams, and J. I. Goldstein, Metall. Trans. **20A**, 719 (1988), and references therein.

[3] D. G. Rancourt and R. B. Scorzelli, J. Magn. Magn. Mater. **150**, 30 (1995), and references therein.

[4] T. Takahashi, W. A. Bassett, and H. K. Mao, J. Geophys. Res. **73**, 4717 (1968).

[5] E. Huang, W. A. Bassett, and M. S. Weathers, J. Geophys. Res. **93**, 7741 (1988).

[6] H. K. Mao, Y. Wu, L. C. Chen, J. F. Shu, and A. P. Jephcoat, J. Geophys. Res. **95**, 21 737 (1990).

[7] R. J. Weiss, Proc. Phys. Soc. London **82**, 281 (1963).

[8] M. Matsui, K. Adachi, and S. Chikazumi, J. Appl. Phys. **51**, 6319 (1980).

[9] S. Chikazumi, J. Magn. Magn. Mater. **10**, 113 (1979).

[10] E. P. Wohlfarth, J. Magn. Magn. Mater. **10**, 120 (1979).

[11] A. Z. Menshikov, Physica B **161**, 1 (1989).

[12] W. J. Carr, Jr., Phys. Rev. **85**, 590 (1952).

[13] M. Dubé, P. R. L. Heron, and D. G. Rancourt, J. Magn. Magn. Mater. **147**, 122 (1995).

[14] M.-Z. Dang, M. Dubé, and D. G. Rancourt, J. Magn. Magn. Mater. **147**, 133 (1995).

[15] D. G. Rancourt, M. Dubé, and P. R. L. Heron, J. Magn. Magn. Mater. **125**, 39 (1993).

[16] Y.-Y. Chuang, Y. A. Chang, R. Schmid, and J.-C. Lin, Metall. Trans. **17A**, 1361 (1986).

[17] B. Dünweg and K. Binder, Phys. Rev. B **36**, 6935 (1987).

[18] G. Inden and W. Pepperhoff, Z. Metall. **81**, 770 (1990).

[19] F. Schmid and K. Binder, J. Phys. Condens. Matter **4**, 3569 (1992).

[20] K. Binder, in *Statics and Dynamics of Alloy Phase Transformations*, edited by P. E. A. Turchi and A. Gonis (Plenum, New York, 1994), p. 467.

[21] R. J. Wakelin and E. L. Yates, Proc. Phys. Soc. London Sect. B **66**, 221 (1953); T. G. Kollie and C. R. Brooks, Phys. Status Solidi A **19**, 545 (1973).

[22] J. Crangle and G. C. Hallam, Proc. R. Soc. London Ser. A **272**, 119 (1963).

[23] E. Josso, J. Phys. Radium **12**, 399 (1951); J. W. Drijver and F. Van der Woude, Phys. Rev. Lett. **34**, 1026 (1975).

[24] J. Paulevé, D. Dautreppe, J. Laugier, and L. Néel, C. R. Acad. Sci. **254**, 965 (1962).

[25] T. Nagata, M. Funaki, and J. A. Danon, in *Memoirs of National Institute of Polar Research Special Issue No. 41, Proceedings of the Tenth Symposium on Antarctic Meteorites* (National Institute

of Polar Research, Tokyo, 1986), p. 364.
[26] I. A. Abrikosov, O. Erickson, P. Söderlind, H. L. Skriver, and B. Johansson, Phys. Rev. B **51**, 1058 (1995).
[27] C. Kuhrt and L. Schultz, J. Appl. Phys. **73**, 1975 (1993).
[28] G. S. Painter, Phys. Rev. Lett. **70**, 3959 (1993).
[29] C. Kittel, *Introduction to Solid State Physics*, 6th ed. (Wiley, New York, 1986), p. 55.
[30] J. B. Staunton, D. D. Johnson, and F. J. Pinski, Phys. Rev. B **50**, 1450 (1994); D. D. Johnson, J. B. Staunton, and F. J. Pinski, *ibid*. **50**, 1473 (1994).